On the Application of Stereographic Projection to the Representation of Moving Targets in Air Traffic Control Systems

Robert G. Mulholland

February 1987

DOT/FAA/CT-TN85/67

Document is on file at the Technical Center Library, Atlantic City Airport, N.J. 08405

U.S. Department of Transportation
Federal Aviation Administration

Technical Center
Atlantic City Airport, N.J. 08405

Technical Report Documentation Page

1. Report No.	2. Government Accession No.	3. Recipient's Catalog No.
DOT/FAA/CT-TN85/67		

4. Title and Subtitle
ON THE APPLICATION OF STEREOGRAPHIC PROJECTION TO THE REPRESENTATION OF MOVING TARGETS IN AIR TRAFFIC CONTROL SYSTEMS

5. Report Date
February 1987

6. Performing Organization Code
ACT-130

7. Author(s)
Robert G. Mulholland

8. Performing Organization Report No.
DOT/FAA/CT-TN85/67

9. Performing Organization Name and Address
Federal Aviation Administration
Technical Center
Atlantic City International Airport
Atlantic City, NJ 08405

10. Work Unit No. (TRAIS)

11. Contract or Grant No.
T0502M

12. Sponsoring Agency Name and Address
U.S. Department of Transportation
Federal Aviation Administration
Advanced Automation Program Office
Washington, DC 20590

13. Type of Report and Period Covered
Technical Note
1984 - 1985

14. Sponsoring Agency Code

15. Supplementary Notes

16. Abstract

In many instances, air traffic control is based on the idea that the latitude and logitude of an aircraft can be represented as a point in a cartesion plane via the method of stereographic projection. In practice, an approximation of this representation is obtained through the processing of measurements of the altitude of the aircraft and its slant range azimuth relative to a radar of known position. The difference between the approximation and the actual representation of aircraft location is viewed as a projection error. In the case of the Advanced Automation System (AAS), the scheduled replacement for the National Airspace System (NAS) design specifications limit the projection errors to 0.005 nautical mile (nmi). Unfortunately, the data processing methods now employed in NAS are insufficient to meet this requirement.

Projection errors in NAS are examined, and methods for reducing them are considered. It is shown how a simple modification of the current NAS methodology can be used to achieve the accuracy imposed on the AAS design.

17. Key Words	18. Distribution Statement
Stereographic Projection Air Traffic Control	Document is on file at the Technical Center Library, Atlantic City International Airport, New Jersey 08405

19. Security Classif. (of this report)	20. Security Classif. (of this page)	21. No. of Pages	22. Price
Unclassified	Unclassified	47	

Form DOT F 1700.7 (8-72) Reproduction of completed page authorized

TABLE OF CONTENTS

EXECUTIVE SUMMARY

Horizontal separation of aircraft under the control of a single Air Route Traffic Control Center in the National Airspace System (NAS) is accomplished by controlling the relative separation of points in a plane that represent actual aircraft locations. Such a representation is supposed to be the image of the orthogonal projection of an aircraft onto the mean sea level surface of the earth under a stereographic mapping. In practice, the system implementation of the mapping is imperfect. Hence, even if the aircraft location is known exactly in terms of surveillance data, i.e., altitude, slant range, and azimuth, there is a difference between the system representation of the aircraft and the image of actual aircraft position under the stereographic mapping. This difference constitutes a projection error, and the magnitude of the error determines how well the system representation of an aircraft reflects its location in terms of latitude and longitude. While the NAS implementation of the stereographic mapping is simple and computationally efficient, the corresponding projection errors exceed limits imposed on the design of the Advanced Automation System (AAS) that is to replace NAS.

The ensuing report examines sources of projection error in NAS. Implementations of the stereographic mapping other than that employed in NAS are considered. Both spherical and ellipsoidal models of the mean sea level surface of the earth are taken into account. An implementation of the stereographic mapping is disclosed that retains much of the simplicity of the NAS design and yet meets the accuracy requirements of the AAS specification in the context of an ellipsoidal earth model.

1. INTRODUCTION.

This report is concerned with projection errors in 2-dimensional representations of airspace employed for air traffic control (ATC) purposes. Some 20 Air Route Traffic Control Centers (ARTCC's) dispersed across the contiguous United States provide ATC services to en route aircraft operating under flight plans filed with the National Airspace System (NAS). The control jurisdiction of a single ARTCC consists of the combined coverage regions of many radars, and involves hundreds of thousands of square miles of the surface of the earth. Range and azimuth data acquired at the radar sites in connection with the location of airborne targets is transmitted to the ARTCC. Additional altitude information is supplied to the ARTCC for those aircraft equipped with Mode C transponders, a mandatory requirement in airspace above 12,000 feet. This surveillance information is used to create a representation of aircraft positions consisting of points in a 2-dimensional coordinate system referred to as the system plane or the ARTCC master plane. Separation of aircraft at the same altitude is effected by controlling the relative positions of the points.

From a theoretical viewpoint, the system representation of a target should be the same as the image of the position of the target above the mean sea level surface of the earth under an explicit mapping of stereographic origin. However, the system implementation of the mapping is imperfect, and measurements of target radar coordinates are rarely exact. As a result, there is a difference between the system representation of the target and the image of target position under the mapping. This difference constitutes a projection error. While there are sources of projection error other than inexact measurements and imperfect implementation of the mapping, they are beyond the scope of this work.

The objective of this report is to disclose some implementations of the projection mapping besides the one created by the designers of NAS. In the case of NAS the implementation is simple and computationally efficient. On the other hand, the corresponding projection errors exceed limits imposed on the design of the Advanced Automation System (AAS) that is scheduled to replace NAS in the next decade. Hence, it is natural to ask how one might alter the NAS implementation without materially destroying the simplicity of the design and yet achieve an accuracy that will meet the needs of the AAS. This report is a step in that direction.

The remainder of the report is divided into 12 sections that deal with projection error in the context of a spherical model of the mean sea level surface of the earth. Extensions to an ellipsoidal model and details of a mathematical nature are relegated to four appendixes. The next three sections review some basic target location parameters and relationships between them that are used in succeeding developments. The projection error can be expected to exhibit some dependance upon target altitude and the position of the target relative to the antenna from which slant range and azimuth are measured. Hence, some quantitative formulation of what is meant by radar coverage region is essential to an analysis of the error. Such a formulation is provided in section 5. The mapping that carries target positions into the master plane can be regarded as a composition of two maps (references 1 and 2). One of these stereographically projects airspace into a so-called local radar plane tangent to the surface of the earth at the latitude and longitude of the radar site from

FIGURE 1. LOCATION PARAMETERS

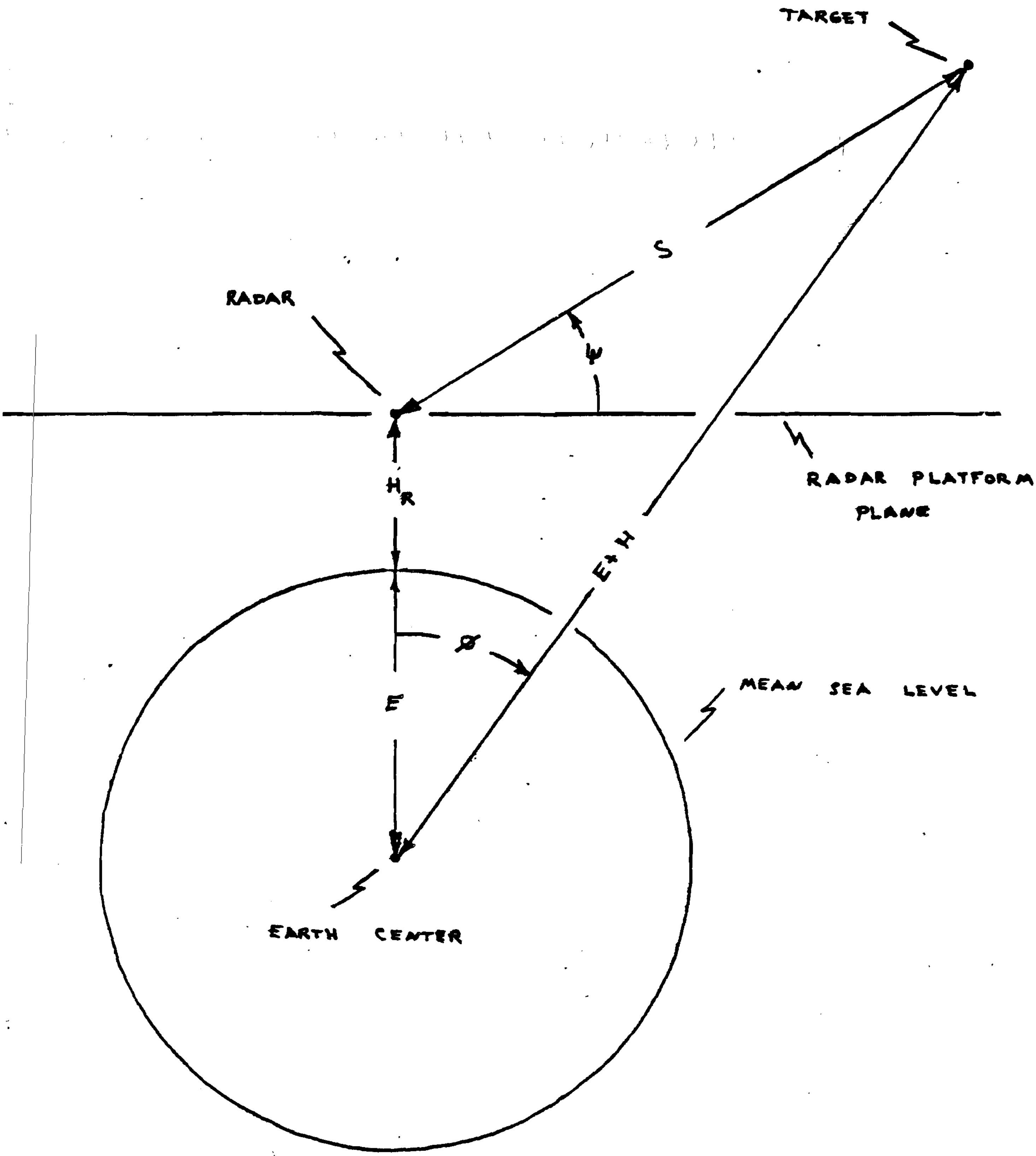

FIGURE 1. LOCATION PARAMETERS

as S increases from 0. Otherwise, it steadily decreases as S increases toward the critical value

$$s_c(\psi) = -(E + H_R) \sin \psi \tag{6}$$

where it takes on its minimum value

$$h_{min}(\psi) = (E + H_R) \cos \psi - E. \tag{7}$$

In fact, at the critical slant range the ψ-elevation surface is tangent to the sphere of radius $E + h_{min}(\psi)$ about the center of the earth. As S continues to increase, the function $h(S, \psi)$ rises, and it passes through H_R as the slant range moves through $2s_c(\psi)$.

The relationship

$$(E + H)^2 = (E + H_R)^2 \cos^2 \psi + [S + (E + H_R) \sin \psi]^2 \tag{8}$$

can be obtained by completing the square in (3). The solution of (8) for slant range leads to the functions

$$s_{lo}(H, \psi) = -[(E + H)^2 - (E + H_R)^2 \cos^2 \psi]^{1/2} - (E + H_R) \sin \psi \tag{9}$$

and

$$s_{hi}(H, \psi) = [(E + H)^2 - (E + H_R)^2 \cos^2 \psi]^{1/2} - (E + H_R) \sin \psi. \tag{10}$$

If ψ is negative and

$$h_{min}(\psi) \leq H \leq H_R \tag{11}$$

then $s_{lo}(H, \psi)$ ($s_{hi}(H, \psi)$) represents the smaller (larger) of the two possible slant ranges for a target on the ψ-elevation surface at altitude H. If either $\psi \geq 0$ or else $\psi < 0$ and the altitude does not satisfy the constraint (11), then $s_{lo}(H, \psi)$ has no physical meaning. On the other hand, when

$$s_{min}(\phi) = (E + H_R) \sin \phi \tag{16}$$

about the antenna, and

$$h_c(\phi) = (E + H_R) \cos \phi - E \tag{17}$$

is the altitude of the locus of the points of tangency. Consequently, there are two possible altitudes for a target on this surface at a slant range S for which

$$s_{min}(\phi) \leq S \leq E + H_R . \tag{18}$$

These are

$$h_{lo}(\phi) = -\left[S^2 - s^2_{min}(\phi) \right]^{1/2} + h_c(\phi) \tag{19}$$

and

$$h_{hi}(\phi) = \left[S^2 - s^2_{min}(\phi) \right]^{1/2} + h_c(\phi) . \tag{20}$$

When S exceeds $E + H_R$ there is only one possible target altitude, and it can be obtained from (20). Slant ranges of this magnitude are not encountered in ATC applications.

In the case where $S \leq E + H_R$, the preceding remarks imply the existance of target locations at slant range S for which the line segment connecting the target to the antenna is perpendicular to the line segment connecting it to the center of the earth. These locations correspond to the circular locus of points defined by the intersection of the sphere of radius S about the antenna and the ϕ-deviation surface that is tangent to the sphere. The altitude of each of these tangency points is given by

$$H_p(S) = \left[(E + H_R)^2 - S^2 \right]^{1/2} - E \tag{21}$$

which can be obtained from obvious geometric considerations or the solution of (16) and (17) for $h_c(\phi)$ in terms of $s_{min}(\phi)$. Obviously, $\phi(S, H_p(S))$ is the maximum deviation angle that can be attributed to a target at slant

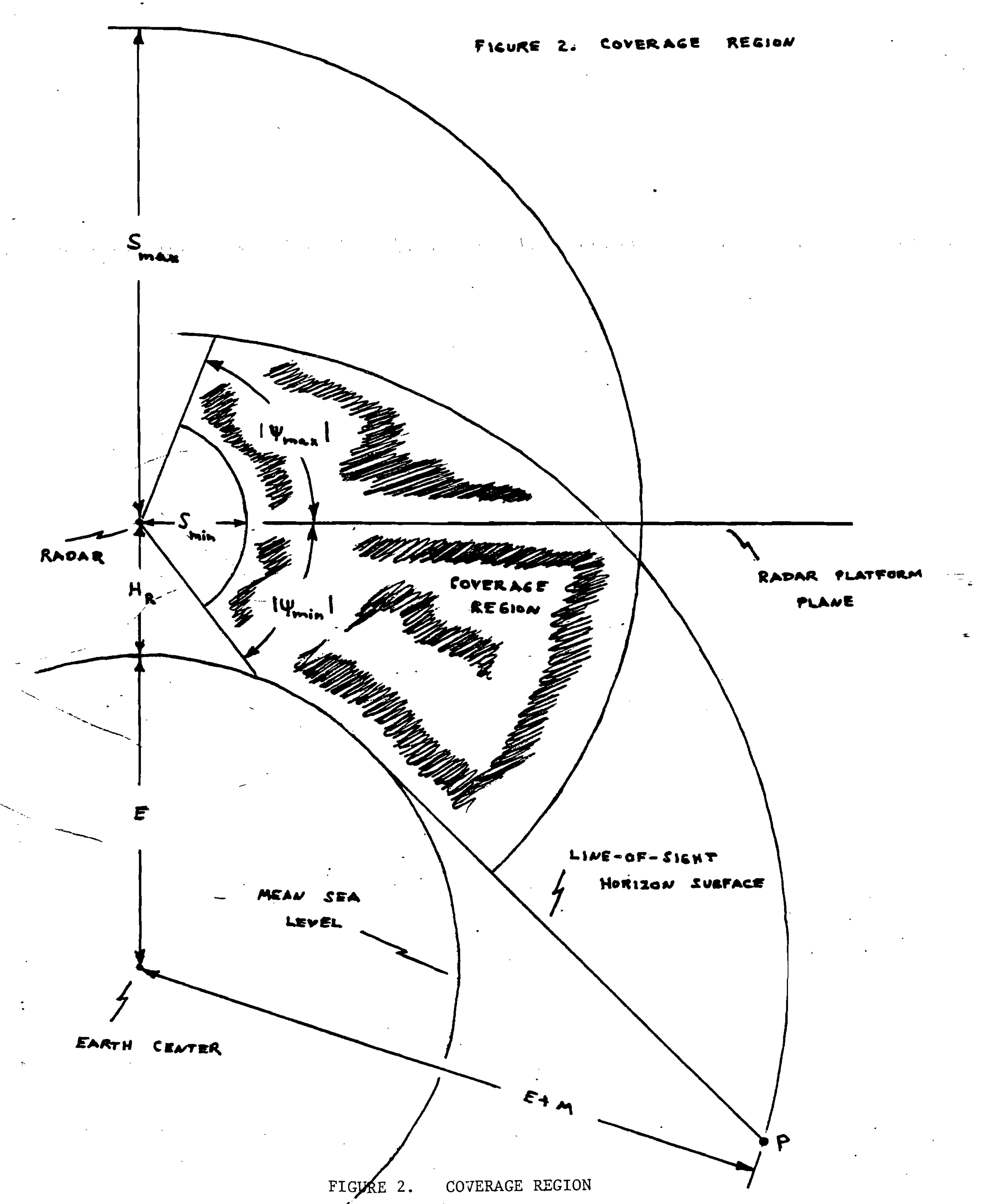

FIGURE 2. COVERAGE REGION

$$0 \leq \Theta < 2\pi. \tag{30}$$

As will be seen, this provides a foundation for evaluating the performance of surveillance techniques based on the method of stereographic projection. For example, there will be subsequent references to the minimum and maximum altitudes $H_{min}(S)$ and $H_{max}(S)$ that can be assumed by a target in the coverage region at slant range S. It can be easily verified that these are provided by the following algorithms in the practical case where ψ_{max} is positive. The algorithms are written in terms of simple PASCAL assignment statements (reference 4) with the understanding that the symbolic representations of mathematical functions on the left (right) side of each expression are to be treated as real varibles (functions).

Algorithm 1. Maximum Altitude

if $(M \leq H_R)$ or $((M > H_R)$ and $(S \geq s_{hi}(M, \psi_{max})))$ then

$$H_{max}(S) = M$$

else

$$H_{max}(S) = h(S, \psi_{max}).$$

Algorithm 2. Minimum Altitude

if $\psi_{min} \geq \psi_0$ then

$$H_{min}(S) = h(S, \psi_{min})$$

else

if $S \geq S_0$ then $H_{min}(S) = h(S, \psi_0)$

else

$$H_{min}(S) = \max(h(S, \psi_{min}), 0).$$

6. STEREOGRAPHIC PROJECTION IN THE LOCAL RADAR PLANE.

A target can be stereographically projected onto any plane tangent to the surface of the earth or, for that matter, tangent to the surface of any sphere about the center of the earth. The phrase "local radar plane" will be used to refer to the plane tangent to the surface of the earth directly beneath the

$$r(S,H) = R(S,H)\left[\alpha(S,H)\right]^{-1/2} \tag{33}$$

where

$$R(S,H) = \left[S^2 - (H-H_R)^2\right]^{1/2} \tag{34}$$

and

$$\alpha(S,H) = \left[1/(2E)\right]^2 \left[(2E+H+H_R)^2 - S^2\right]. \tag{35}$$

Thus, target slant range, altitude, and azimuth can be used to compute the complex representation $z(S, H, \theta)$ of the stereographic projection of the target onto the local radar plane via (31) and (33).

7. GROUND RANGE ESTIMATION WHEN ALTITUDE IS UNKNOWN.

Let $\phi_{min}(S)$ ($\phi_{max}(S)$) represent the minimum (maximum) deviation angles that can be attributed to a target in the coverage region at slant range S from the antenna. It follows from (32) that

$$r_m(S) = E\left\{\tan\left[\phi_{max}(S)/2\right] + \tan\left[\phi_{min}(S)/2\right]\right\} \tag{36}$$

is the arithimetic mean of the maximum and minimum ground ranges that can be associated with such a target. Moreover, the maximum value of the difference between $r_m(S)$ and the true ground range of the target is

$$e_m(S) = 2E\tan\left[\phi_{max}(S)/2\right] - r_m(S). \tag{37}$$

Thus, when target altitude is known only to the extent that it lies between the minimum and maximum altitudes $H_{min}(S)$ and $H_{max}(S)$ that can be attributed to a target in the coverage region at slant range S, then $r_m(S)$ can be used as an estimator of target ground range, and the absolute value of the corresponding estimation error cannot exceed $e_m(S)$. This estimator is optimal in the sense that the maximum error associated with any other estimate of ground range cannot be less than $e_m(S)$.

viewed as an attempt to approximate $r_m(S)$. However, in the case where the slant range exceeds $s_{hi}(M, \psi_{max})$, a much closer approximation can be obtained from a least squares fit of a low order polynomial function of 1/S to samples of $r_m(S)$. In the cases where the slant range falls below $s_{hi}(M, \psi_{max})$, our experience indicates that $r_m(S)$ is essentially a linear function of S. However, there is a problem with polymomial fitting in the sense that $r_m(S)$ does change with the configuration of the coverage region, and so one cannot expect the same pair of polynomials to apply to all radar sites in NAS. Thus, one is left with the usual problem of deciding whether the benefit to be derived from optimality is worth the effort needed to achieve it.

8. GROUND RANGE ESTIMATION WHEN ALTITUDE IS KNOWN.

When both altitude and slant range are known, the ground range can be obtained from (33). However, there are many ways in which this computation can be carried out. To the extent that computational speed and consumption of computational resourses are important, some of these may be desirable and others not so desirable. In what follows, an approach to the determination of ground range will be described that is easy to implement in a form that provides quick results accurate to within 2 m.

There exist efficient high speed techniques (reference 6 and 7) for evaluating the factor R(S, H) in the formula (33) for ground range. The remaining factor can be expressed as a polynomial in x(S, H) by a straight forward application of Taylor's theorem with a remainder to the expansion of the reciprocal of the square root of x about an arbitrary positive number x_o. In other words, the ground range can be expressed in the form

$$r(S, H) = r_m(S, H, x_o) + e_m(S, H, x_o, \xi) \tag{42}$$

where ξ is a number between x_o and x(S, H),

$$r_m(S, H, x_o) = R(S, H) \sum_{k=0}^{m} [D_k(x_o)/m!][x(S, H) - x_o]^m, \tag{43}$$

$D_k(t)$ is the k th derivative of $(1/x)^{\frac{1}{2}}$ evaluated at x = t, and

$$e_m(S, H, x_o, \xi) = R(S, H)[D_{m+1}(\xi)/(m+1)!][x(S, H) - x_o]^{m+1}. \tag{44}$$

Thus, if $r_n(S, H, x_o)$ is used to estimate the ground range then the corresponding estimation error is given by (44). Unfortunately, ξ is unknown and so the error cannot be evaluated. On the other hand, it is possible to find an upper bound on the absolute value of the error that is valid for any pair (S, H) corresponding to a target location in the coverage region, and, in the case of NAS, this bound is on the order of a meter when both x_o and n are assigned the value 1. As a result, the estimator and

$$M \leq 60{,}000 \text{ ft} \tag{52}$$

are satisfied throughout NAS. Hence, by using the right sides of constraints (50)-(52) in place of S_{max}, H_R, and M in (46)-(49) an upper bound on the estimation error can be obtained that is valid for all radar coverage regions in NAS. For example,

$$|r_0(S, H, 1, \xi)| \leq 630 \text{ m} \tag{53}$$

and

$$|r_1(S, H, 1, \xi)| \leq 1.60 \text{ m}. \tag{54}$$

From (54) it is concluded that $r_1(S, H, 1)$ is essentially the same as the ground range over the coverage region of any radar site in NAS. On the other hand, the same conclusion cannot be drawn for $r_0(S, H, 1)$ from (53).

Although the projection error associated with the estimate (45) is negligible in the context of a spherical earth model, it does not necessarily follow that the same will be true in the context of an ellipsiodal model. However, there does exist an interesting possibility for employing the estimator (45) as a means for essentially eliminating the projection error when the earth is represented by the reference ellipsoid. This subject has already been touched on in the open literature (reference 2), and the main features of the idea are provided in appendix C.

9. STEREOGRAPHIC RELATIONSHIPS.

As already pointed out, an ARTCC is serviced by a multitude of radars, and control of aircraft in the horizontal sense is effected through stereographic representations of target locations in a single plane. This center master plane is tangent to a so-called conformal sphere. The center of the sphere is collocated with the center of the earth. However, the radius need not be the same as that of the earth. Target representations in the master plane are obtained from the stereographic representations of the targets in the local planes associated with the radars that support the ARTCC. For example, using appropriate coordinate systems in the local and master planes with origins at the points of tangency, the master plane representation of a target associated with the complex number z in a local radar plane is given by

$$w = w_0 + [A + B|w_0|^2] z [1 - B w_0^* z]^{-1} \tag{55}$$

10. PROJECTION ERROR IN MASTER PLANE.

Suppose now that z_e is the estimate of the stereographic representation of the target in the local radar plane. For example, it might be the product of $r_n(S, H, x_o)$ and the phasor $\exp(i\,\theta)$. Also supppose that $w_N(E_x, z_e)$ is used to estimate the stereographic representation of the target in the master plane. Then

$$g_N(E_x, z_e) = w_N(E_x, z_e) - w \tag{59}$$

represents the corresponding projection error. Using (55) and (58), it follows that

$$g_N(E_x, z_e) = [A + B|w_o|^2][(E/E_x) z_e D - z C] \tag{60}$$

where

$$C = [1 - B w_o^* z]^{-1} \tag{61}$$

and

$$D = \frac{1 - [(E/E_x) w_o^* B z_e]^N}{1 - (E/E_x) w_o^* B z_e} . \tag{62}$$

Clearly, (60) cannot be obtained from (59) in the event that either of the factors w_o^*Bz and $(E/E_x)w_o^*Bz_e$ is one. As already indicated, this is not a problem in the case of the former factor, and, as will be shown, the same is true in the case of the remaining term. While formula (60) is exact, it does not provide much insight into the relationship between z_e, E_x, and the projection error. In what follows, consideration will be given to an approximation that does provide such insight.

In practical situations both C and D are close to unity. Consequently, one is tempted to conclude that the projection error can be closely approximated by

$$\tilde{g}(E_x, z_e) = [A + B|w_o|^2][(E/E_x) z_e - z] . \tag{63}$$

Unfortunately, this is not necessarily true. For instance, one can construct practical examples for which the absolute value of the difference between or 200 nmi so long as the target is within the coverage region of the radar. On the other hand, the reciprocal of L is typically on the order of thousands of nmi. Consequently, the second restriction is not a serious impediment to the validity of the bound. Incidently, (67) together with the fact that the radius E of the spherical earth model must be between a and b implies that the magnitude of the factor $(E/E_x)w_o{*}Bz_e$ is less than 1. Thus, as indicated before, there is little reason to be concerned with the indeterminate situation in connection with the expression (60).

When the order of the approximation is 1 the bound is given by

$$U = [E_r/b + |w_o| L] L^2 |z|^3 [1 - L|z|]^{-1}. \tag{68}$$

When N exceeds 1 it is given by

$$W = F|\hat{g}_N(E_x, z_e)| + U \tag{69}$$

where

$$F = \frac{L|z|[1 + \rho(1 - L|z|)]}{(1 - L|z|)(1 - \rho L|z|)} \tag{70}$$

and ρ is any number satisfying the inequality

$$(a/E_x)(|z_e|/|z|) \le \rho < 1/(L|z|). \tag{71}$$

The existence of ρ is guaranteed by the restriction (67). Moreover, since F is an increasing function of ρ it is clear that the same is true of the bound W., i.e., the bound is tightest when ρ is set equal to the left most member of (71). For future reference it is pointed out that the definition (66) of L implies that both U and F increase monotonically with $|w_o|$ and $|z|$ so long as the constraint (65) on $L|z|$ is satisfied. An example will show how this monotonicity can be used to evaluate the accuracy of our approximation of the projection error.

The accuracy of the approximation (64) will be illustrated in the context of the En Route Automated Radar Terminal System (EARTS) mosaic model for Alaska (reference 8). According to the model, there are 15 radars supporting the ARTCC, the radius E_r of the conformal sphere is 3395.7 nmi, the maximum effective slant range of each radar is no more that 200 nmi, and the distance of the stereographic representation of each site in the master plan from the point when the approximation is expressed in m. Consequently, when the approximation order is greater than 1 the magnitude of the error is at most 7.04 m plus about one percent of the magnitude of the approximation itself. Clearly, the accuracy of the approximation (64) is pretty good.

For the most part, one is interested in the magnitude of the projection error and so it is convenient to have a simple expression for the magnitude of $g_N(E_x, z_e)$. Such an expression is easy to derive in the practical case where the phase of the estimate z_e is the complement of the target azimuth θ. Then, at least in the context of a spherical earth model, the phases of z and z_e are identical. Since (56) and (57) imply that the phases of A and B are always the same, namely, $-\beta$, it follows from (63) that the magnitude of the expression (64) is invariant to azimuth when the approximation order exceeds 1. On the other hand, when the order of approximation is 1 it is apparent that the magnitude varies with azimuth and is maximum when the azimuth is π radians out of phase with the complement of the sum of β and the phase of w_o. As a result,

$$|\tilde{g}(E_x, z_e)| = [\,|A| + |B|\,|w_o|^2\,]\,\big|\,(E/E_x)\,|z_e| - |z|\,\big| \tag{76}$$

and

$$\max_{\theta} |\hat{g}_N(E_x, z_e)| = \begin{cases} |\tilde{g}(E_x, z_e)| + [\,|A| + |B|\,|w_o|^2\,]\,|w_o B|\,|z|^2 & \text{if } N = 1 \\ |\tilde{g}(E_x, z_e)| & \text{if } N > 1 \end{cases} \tag{77}$$

whenever the phase of the estimate of the stereographic representation of the target in the local radar plane is the complement of target azimuth.

The relationship (77) can be used to illustrate the importance of the distinction between the radius of the earth and that of the conformal sphere in the transformation (55) relating the stereographic representations of the target in the local radar plane and the master plane. In particular, great pains were taken by the designers of NAS to make the ground range estimate $|z_e|$ as close as possible to the true ground range $|z|$ of the target. However, even if the true ground range and its estimate are the same, a poor choice for E_x in the approximation (58) can cause projection errors on the order of a nmi. For example, suppose the radius of the conformal sphere is assigned to E_x as is the current practice in NAS. Then

$$\max_{\theta} |g_N(E_x, z_e)| \geq |\tilde{g}(E_x, z_e)| \geq \left[\frac{E_r}{E} + \frac{|w_o|^2}{4E_r E}\right] \left|\frac{E}{E_r} - 1\right| |z| \tag{78}$$

when the estimate $|z_e|$ of ground range is exact. In terms of the Alaskan where

$$\Delta x = [C_S \Delta S + C_H \Delta H] \sin\theta + r_1(S, H, 1) \Delta\theta \cos\theta, \tag{82}$$

$$\Delta y = [C_S \Delta S + C_H \Delta H] \cos\theta - r_1(S, H, 1) \Delta\theta \sin\theta, \tag{83}$$

and C_S (C_H) is the partial deriviative of $r_1(S, H, 1)$ with respect to S (H) evaluated at the actual slant range and azimuth of the target. This expression can be viewed as a first order approximation of the error in the estimate of the actual stereographic representation of the target in the local radar plane due to measurement errors. This is not the total projection error. The total error is given by

$$e_L = \mu(S, H, \theta) + Z_e(S+\Delta S, H+\Delta H, \theta+\Delta\theta) - Z_e(S, H, \theta) \tag{84}$$

where

$$\mu(S, H, \theta) = Z_e(S, H, \theta) - z \tag{85}$$

is just the projection error in the case for which the measurements are exact. To the extent that the first order approximation of the component of the error due to inexact measurement is valid, the total error in the local plane can be represented by the sum of $\mu(S, H, \theta)$ and Δz_e. Needless to say, the magnitude of the former is just the absolute value of the difference between the true ground range of the target and $r_1(S, H, 1)$. As already pointed out in section 8, this is, at most, a few meters for coverage regions of the type encountered in ATC applications.

The projection error in the master plane can be approximated by substituting e_L for z_e in formula (64). As already demonstrated, the approximation error associated with this formula is negligible for current ARTCC control jurisdictions. Also, as pointed out early, it is good design practice to assign the radius of the earth to E_x regardless of the order N of the polynomial that is used to map the local plane into the master plane. With this understanding, the total projection error in the master plane associated with the Nth order transformation polynomial can be represented by length $\lambda\sigma_1$ lies along the line segment connecting the representation of the target and the antenna in the local radar plane. The result is

$$P(\lambda) = 1 - \varepsilon^{-(\lambda^2/2)} \quad . \tag{91}$$

It is left to the reader to derive a similar relationship for the master plane from the relationship (86).

It is emphasized that (91) is based on the assumption that (81) does indeed qualify as an accurate approximation of the difference between $Z_e(S+\Delta S, \Delta H+H, \theta+\Delta\theta)$ and $Z_e(S, H, \theta)$. Clearly, this is not the case when the measurement errors are large. Consequently, one might do well to at least demonstrate the validity of the relationship before using it as a design tool.

12. CONCLUSIONS.

There are many ways of going about estimating target ground range in the local radar plane in the case where altitude is unknown. The approach to ground range estimation described in this report is optimal in the minimax sense. The current method employed in NAS is optimal in the same sense only in the context of a flat earth model. It is, at best, suboptimal in the context of a spherical model.

While ground range can be determined exactly when altitude is known, it has been shown here that computations can be greatly simplified by resorting to an approximation of the exact formula that is accurate to within 2 m for any target in the coverage region of the radar. This, together with a special method for calculating the difference between S^2 and $(H-H_R)^2$, can be used to formulate an efficient, high speed algorithm for estimating the stereographic representation of the target in the local plane. Numerical studies (appendix C) indicate the existence of extensions of the algorithm to the ellipsoidal earth model for which the projection error can be essentially eliminated under the geometric limitations imposed by ARTCC control jurisdictions and ATC radar coverage regions of practical import. One of these extensions involves a ground range correction factor that limits the ground range error to values less than 5 m. The corresponding error in phase involves angles that are less than 0.006°. These bounds are cosiderably less than the slant range and azimuth quantization intervals of 0.0078 nmi and 0.022° associated with the Mode S system that is scheduled to replace the current operational ATC radar beacon system. Unfortunately, at ground ranges of 200 nmi from the antenna the phase error can lead to projection errors on the order of 0.02 nmi which exceeds the 0.005 nmi limit imposed on projection errors by current AAS requirements. However, by introducing a phase correction factor in addition to the ground range correction, it is possible to hold the projection errors in both the local radar plane and the ARTCC master plane to levels that are well within AAS specifications. In fact, this can be accomplished in such a manner that the master plane magnification factor (reference 2) is optimized. Insofar as size of the control jurisdiction is concerned, the 2500 x 2500 nmi limitation imposed by the AAS specification on the surveillance coverage region of the Area Control Computer Complex does not present an obstacle to successful application of the range and phase correction factors.

REFERENCES

1. Mulholland, R. and D. Stout, Numerical Studies of Conversion and Transformation in a Surveillance System Employing a Multitude of Radars, Part I and II, Astia Documents AD A072-085 and 086, National Technical Information Service, Springfield, VA, April 1979.

2. Mulholland, R. and D. Stout, Stereographic Projection in the National Airspace System, IEEE Transactions on Aerospace and Electronic Systems, January 1982.

3. Abramowitz, M. and I. Stegin, Handbook of Mathematical Functions, National Bureau of Standards, Washington DC, 1966.

4. Koffman, E., Problem Solving and Structured Programming in PASCAL, Addison Wesley, Reading, MA, 1981.

5. Saleh, N., A. Smith, B. Sokkappa, The Stereographic Projection in the National Airspace System: Principles, Approximations, and Errors, MTR-83W67, The MITRE Corporation, Mc Lean, VA, May 1983.

6. Stout, D., and R. Mullholland, Design and Implementation of Efficient Algorithms for Automatic Determination of Corrected Slant Range, Report No. DOT/FAA/CT-81/30, February 1982.

7. Stout, D., and R. Mulholland, Approximation of Corrected Slant Range in a Radar Surveillance System, IEEE Transactions on Aerospace and Electronic Systems, September 1981.

8. Test Report for EARTS Tracking Improvement, Contract FAA No. DTFA01-84-C-00007, NAS Modernization - En Route Automated Radar Tracking System with Mosiac Software (EARTS-M), Sperry Corporation, July 1984.

9. Advanced Automation System, System Level Specification, Design Competition Phase, FAA-ER-130-005E, August 1984.

APPRENDIX A

SLANT RANGE EXTREMUM IN THE ALTITUDE WINDOW

Let J represent the set of points in the intersection of the beam and the window comprising all altitudes from 0 to M. Suppose there are targets in J at altitude H. Since slant range increases with increasing deviation angle at constant altitude it follows that among all such targets the one with the greatest deviation angle will be farthest from the radar.

Now consider the case where ψ_{min} is less than the elevation angle of the line-of-sight horizon. Clearly, the target at altitude H in J at the greatest distance from the antenna must lie on the ψ_o-elevation surface, and the corresponding slant range is $s_{hi}(H,\psi_o)$. But formula (10) implies this is an increasing function of altitude. Hence, the greatest distance S_1 between the antenna and a point J must be $s_{hi}(M, \psi_o)$. In like manner, it can be shown that S_1 is $s_{hi}(M, \psi_{min})$ when $_{min} \geq \psi_o$.

Finally, since the slant range of a constant altitude target decreases with decreasing deviation angle, $s_{hi}(M, \psi)$ is a decreasing function of elevation angle, and so $s_{hi}(M, \psi_o)$ exceeds $s_{hi}(M, \psi_{min})$ if, and only if, $\psi_{min} > \psi_0$. Thus, in general, S_1 is given by (25).

APPENDIX B

ERROR BOUND

Consider any pair (S, H) corresponding to a target in the coverage region. Expression (34) implies that R(S, H) cannot exceed the maximum slant range S_{max} of the radar. Moreover, as will be seen, x(S, H) is bounded above by v and below by u. Also, the magnitude (47) of the (n+1)th derivative of $1/\sqrt{t}$ is a decreasing function of t. Consequently, (46) must be an upper bound for $e_n(S, H, x_o, \xi)$.

In order to establish u as a lower bound for x(S, H) one need only note that S_{max} is certainly less than the polar radius of the earth in ATC applications and the latter is not greater than E. Consequently, (35) implies

$$x(S, H) \geq 1 - [S_{max}/(2E)]^2 \geq u. \tag{B-1}$$

The upper bound v can be obtained from (35) and the fact that M is the maximum target altitude in the coverage range, i.e.,

$$x(S, H) \leq [1/(2E)]^2 (2E + M + H_R)^2 \leq v. \tag{B-2}$$

APPENDIX C

ELLIPSOIDAL EARTH MODEL

Under the assumption of an ellipsoidal earth model the altitude of a point above mean sea level is the distance separating the point from its orthogonal projection onto the ellipsoidal surface. The geodetic coordinates of a target at altitude H are specified in terms of the triplet (L, λ, H) where L and λ are the geodetic latitude and the longitude of the target. The latitude measures the angular deviation from the equatorial plane of the normal to the ellipsoidal surface at the projection of the target. Thus, it specifies the location of the projection to within a circle about the polar axis of the earth. The longitude represents an angle measured in the plane through the circular locus from the projection to a fixed half plane defined by the polar axis and a predetermined point on the surface of the earth. As a result, latitude and longitude uniquely specify the projection of the target on the surface of the earth and this, together with altitude, provides the location of the target itself.

If it is imagined that the lengths of the axes of the ellipsoid approach one another, then L approaches the angular deviation from the equatorial plane of the line segment connecting the target to the center of the earth. In fact, points on the ellipsoid are often associated with points on the surface of a so-called conformal sphere about the center of the earth. Specifically, the point $(L, \lambda, 0)$ on the ellipsoidal surface is equated to the point on the surface of the sphere at longitude λ and latitude $\nu(L)$ where

$$\nu : L \rightarrow \phi \tag{C-1}$$

is the mapping defined by the equation

$$\left[\frac{1-\epsilon \sin L}{1+\epsilon \sin L}\right]^{\epsilon/2} \tan\left[\pi/4 + L/2\right] = \tan\left[\pi/4 + \phi/2\right] \tag{C-2}$$

and ξ is the eccentricity of the ellipsoid (references 1 and 2). The angle $\nu(L)$ is sometimes referred to as the conformal latitude of the target. As will be seen, this concept bears directly on the definition of the local radar plane in the context of an ellipsoidal earth model.

Consider a radar with geodetic coordinates (L_s, λ_s, H_R). The antenna axis corresponds to the normal to the ellipsoidal surface at $(L_s, \lambda_s, 0)$, and rotation is commonly in the direction counter to that dictated by the right hand rule with respect to the direction along the axis at the radar away from the ellipsoid. The azimuth of a target is determined by two half planes having the as the range and phase components of the error. If the lengths of the semi-minor and major axes of the ellipsoid approach the common value E, then (C-4) reduces to the projection error in the context of the spherical model, the angle error vanishes, and, as pointed out in section 8, the range error is negligible for radar coverage regions like those encountered in practical ATC applications. However, it still remains to show how the projection error for such coverage regions can be neutralized in the situation where the mean sea level surface of the earth is represented by the reference ellipsoid.

If we employ the reference ellipsoid as the earth model and assume that the coverage region of the radar is constrained by inequalities (50) - (52), then the range and phase components of the projection error can be represented by sinusoidal functions of the phase of the true representation z of the target in the local radar plane with amplitudes that vary with the magnitude of the representation. In particular, consider the case where z is constrained to lie on a circle about the point of tangency of the local radar plane, target altitude is held constant, and the phase of z is increased from 0 to 2π radians. Empirical data (references 1 and 2) suggest that both the range and phase errors oscillate in an almost sinusoidal like manner. The same data also suggest that the amplitude of the range (phase) error oscillation is a nearly quadratic (linear) function of the radius of the circle. Although the ampitudes of the oscillations do vary with the geodetic latitude of the radar site, the radar site altitude, and the altitude of the target, the variation with target altitude is extremely small over the values assumed by this parameter in ATC applications. In more explicit terms, empirical data suggest that the approximations

$$\delta_2(z, H) \approx [a_0 + a_1|z| + a_2|z|^2] \sin[\arg(z)] \qquad \text{(C-7)}$$

and

$$\delta_3(z, H) \approx [b_0 + b_1|z|] \sin[\arg(z) - \pi/2] \qquad \text{(C-8)}$$

are highly accurate representations of the range and phase components of the projection error where the coefficients a_0, a_1, a_2, b_0, and b_1, are functions of the radar site latitude L_s and the radar site altitude H_R.

The coefficients a_0 through b_1, can be determined by applying least squares methods to samples of the range (phase) errors corresponding to a single target altitude and a sequence of values of z along the positive half of the imaginary (real) axis of the local plane coordinate system where arg(z) is $\pi/2$ (0) radian. The target altitude chosen for this task might be half the maximum altitude of interest within the coverage region of the antenna. For example, into the master plane. The answer to this question is affirmative. In particular, the reader need only refer to the formula provided in reference 1 for the impact of the projection error in the local plane on the corresponding error in the master plane. A little thought will lead to the conclusion that the projection error in the master plane associated with the use of (C-9) and (C-10) in the estimation of the local plane representation of the target is essentially the same as the corresponding error in the local plane under the usually constraints imposed on the geometry of an ARTCC control jurisdiction. The recent numerical work performed at the FAA Technical Center substantiates this conclusion for cases where the radar site is located at distances up to 1460 nmi from the latitude and longitude marking the so-called master plane point of tangency.

It is emphasized that the accuracies claimed for the estimates (C-9) and (C-10) are based on empirical data rather than a mathematical derivation. Moreover, the data were collected for selected radar site latitudes in the northern hemisphere for which the coverage region of the antenna does not include the north pole or the equator. We do not expect the relationships (C-9) and (C-10) to hold for radar sites near a pole for which the coverage region involves points on the surface of the ellipsoid on both sides of any plane passing through the polar axis. Likewise, these approximations cannot be expected to be valid for sites in the neighborhood of the equator where the coverage region involves portions of the earth'surface in both the northern and southern hemispheres.

Finally, the projection error in the master plane is dependent upon the corresponding error in the local plane as well as the bilinear transformation used to map the latter plane into the former. The transformation is itself a function of E and another parameter E_r that is sometimes referred to as the radius of the conformal sphere supporting the master plane (references 1 and 2). If E_r is improperly evaluated, then there is no guarantee that the projection error in the master plane will be commensurate with that in the local plane. This problem can be avoided by choosing E_r to optimize the so-called magnification factor in accord with the method outlined in reference 2. In fact, no difficulty whatsoever should be encountered for the control jurisdiction geometries cited in the AAS specification, and there is good reason to believe that the approach to the projection problem outlined in this appendix can be successfully applied to the case where the size of the jurisdiction is extended well beyond the limits prescribed by the specification for the surveillance coverage region of the Area Control Computer Complex.

$$\tilde{g} = [A + B|w_0|^2][1/(w_0^* B)][y - x] \tag{D-6}$$

corresponds to (63) and

$$u = [A + B|w_0|^2][1/(w_0^* B)][x^3/(1-x)]. \tag{D-7}$$

By expressing x as a function of z through (D-1) and using the fact that E lies between a and b, it can be verified that $|u|$ is upper bounded by U of (68).

Turning to the case where N exceeds 1, it will be noted that

$$\sum_{k=1}^{N} (y^k - x^k) = y - x + (y - x) f(x, y) \tag{D-8}$$

where

$$f(x, y) = \sum_{k=2}^{N} g(x, y) \tag{D-9}$$

and

$$g(x, y) = \sum_{l=0}^{k-1} y^l x^{k-1-l}. \tag{D-10}$$

As a result, (D-4) can be written as

$$g_N = \tilde{g} + f(x, y)\tilde{g} - v \tag{D-11}$$

where

$$v = [A + B|w_0|^2][1/(w_0^* B)][x^{N+1}/(1-x)]. \tag{D-12}$$

Under the constraint (65) the magnitude of v is upper bounded by that of u. Hence, U of (68) must upper bound $|v|$. Thus, to establish the validity of the bound (69) it only remains to verify the inequality

$$|f(x,y)| \leq F. \tag{D-13}$$

Toward achieving the last stated goal we point out that

$$|g(x,y)| \leq \sum_{l=0}^{k-1} |y|^{l} |x|^{k-1-l}. \tag{D-14}$$

Moreover, by multiplying the leftmost inequality of the relationship (71) through by $|w_0 * B|$ and recalling that the radius of the spherical earth model cannot exceed a, it is apparent that

$$|y| \leq \rho |x|. \tag{D-15}$$

Consequently,

$$|g(x,y)| \leq |x|^{k-1} \sum_{l=0}^{k-1} \rho^{l} = \begin{cases} k|x|^{k-1} & \text{if } \rho = 1 \\ \dfrac{(1-\rho^{k})|x|^{k-1}}{1-\rho} & \text{if } \rho \neq 1 \end{cases} . \tag{D-16}$$

From this relationship and the obvious inequality

$$|f(x,y)| \leq \sum_{k=2}^{N} |g(x,y)| \tag{D-17}$$

the objective can be achieved.

In what follows, we verify (D-13) for the case where ρ is not one. Verification of the inequality for the remaining case is left to the reader. When ρ is other than one the relations (D-16) and (D-17) imply